Progress In Electromagnetics Research M, Vol. 109, 113–123, 2022

A CPW Fed Cross-Shaped Dual-Band Circularly Polarized Monopole Antenna with Strip/Stub/Slot Resonator Loadings

Monika Jangid[1], Jaiverdhan[2, *], Sanjeev Yadav[3], and Mahendra M. Sharma[4]

Abstract—A new compact CPW fed dual-band circularly polarized (CP) antenna for a broadcasting satellite application is presented. The proposed dual-band CP antenna consists of a modified CPW ground structure by loading stub/slots/inverted L-strip and a modified cross-shaped patch. A modified CPW ground structure is able to generate circular polarization. The proposed antenna design provides the simulated impedance bandwidth (IBW) ($S_{11} < -10$ dB) of 81.42% (3.16–7.5 GHz) and 20.53% (11.8–14.5 GHz), respectively, and the 3-dB axial ratio BW (3-dB ARBW) for two bands are 29% (4.18–5.6 GHz) and 8.86% (11.86–12.96 GHz), respectively. The proposed CP antenna provides a maximum gain about 3.8 dBi and 5 dBi in lower and upper bands, respectively, with right-hand circular polarization (RHCP) radiations. The overall size of the CP antenna is $27 \times 27 \times 1\,\text{mm}^3$.

1. INTRODUCTION

In the present scenario, there is a huge demand for circularly polarized antennas in wireless systems such as satellite and mobile communications. Modern communication requires compact size antennas with large bandwidths [1]. It is a challenging task to get wider bandwidth with compact size, and few reported antennas satisfy this type of challenge. Antenna polarization shows the polarization of the radiated wave of the radio antenna toward that path [2, 3]. On the off chance that the heading is not articulated, polarization is considered to be the polarization toward maximum gain. The main feature of a CP antenna is independent from the alignment of the E.F. vector at both receiving and transmitting sides, and due to this feature, it avoids the polarization mismatch losses that occur in the case of linear polarization [4, 5]. In mobile communication constant orientation is an important aspect that is not easily maintained by the linear polarized antenna, so to maintain it, CP is a good choice because with CP, received signal strength is constant with antenna orientation. Besides the above advantage, CP antenna also provides a reduction of Faraday rotation effect that is responsible for the loss of signal (approximately 3 dB or more) if linear polarization is used [6–9]. The utilization of circularly polarized antenna presents a satisfying response for accomplishing this polarization coordinate which takes into consideration greater adaptability in the edge among transmitting and receiving antennas, lessens the impact of multipath reflections, upgrades climate entrance, and takes into consideration the portability of both the transmitter and receiver. Circular polarization can be characterized by three parameters: 3-dB ARBW which is the fraction of the major axis to the minor axis, sense of rotation (RHCP or LHCP), and tilt angle. The value of AR for the CP antenna should be less than 3 dB in the operating frequency band. Coplanar waveguide (CPW) feed provides the advantages like diminished radiation losses, lesser dispersion, and simple integration. Polarization reversal occurs when the signal is reflected from the ground that is RHCP reflections showing LHCP [2].

Received 22 December 2021, Accepted 17 March 2022, Scheduled 1 April 2022

* Corresponding author: Jaiverdhan (jaiverdhan@ieee.org).

[1] Napino Auto & Electronics Ltd Manesar, India. [2] Department of ECE, JECRC, Jaipur, Rajasthan, India. [3] Department of ECE, GWEC, Ajmer, Rajasthan, India. [4] Department of ECE, MNIT, Jaipur, Rajasthan, India.

Various techniques have been reported in the literature based on single feed and/or dual feed, loading passive components like chip register, capacitors, and stub/slot/slits resonating structures to create perturbation in the path of the electric field which excites two orthogonal current modes of the same magnitude and quadratic phase difference (PD). Moreover, these techniques possess limitations of either linearly polarized (LP) [10, 11] or narrow bandwidth, complex geometry, and difficulty to realize with monolithic microwave integrated circuits (MMICs) [12–16].

In this paper, a dual-band CPW feed CP antenna is designed which is compact, easy to design, low cost (designed over an FR-4 substrate), and provides wide dual-band IBW and 3-dB ARBW. The circular polarization is achieved due to two stubs that are provided on the ground plane. Further improvement in 3-dB ARBW and IBW is achieved by cutting slots on the right side of the ground and by providing stubs on the left side. In the proposed antenna dual-bands are achieved due to the square stub at the lower side of the ground structure. It provides wide bandwidth with good radiation characteristics (RHCP) in the broadside direction of the antenna.

2. DESIGN CONFIGURATION AND ANALYSIS OF ANTENNA

2.1. Antenna Geometrical Configuration

The geometrical configuration of the dual-band CPW fed CP antenna with stub and strip loaded ground structure is depicted in Fig. 1. FR-4 substrate material is used for designing the antenna, which has dielectric constant ($\varepsilon r = 4.3$) and loss tangent ($\tan\delta = 0.002$) with the overall floor area (Length (L) $\times$ width (W) being $27 \times 27\,\text{mm}^2$ and thickness (h) of 1 mm. To calculate the dimension of the CPW standard design equations are used. Massive simulations are carried out using CST Microwave Studio (CST MWS) (which is based on finite integration technique (FIT) [17]) to optimize the design parameters of the designed antenna. The optimized dimensions of the designed antenna are given in Table 1.

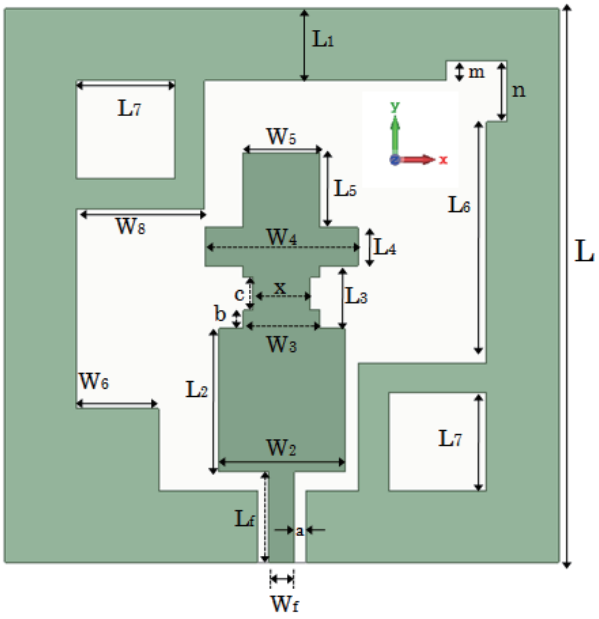

Figure 1. Geometry of proposed CP antenna.

2.2. Design Analysis

The design stages of the CP antenna are completed in five different steps as depicted in Fig. 2. In stage I, the square ground is used with a modified patch. In this design, a rectangular patch is modified by the embedded stair-like shape at the top of the patch. It provides wideband IBW in a single band

Table 1. Optimized design parameters.

Parameter	Value (mm)	Parameter	Value (mm)	Parameter	Value (mm)
$\mathbf{W_5}$	3.73	$\mathbf{W_2}$	6.14	$\mathbf{W_6}$	3.8
$\mathbf{L_1}$	3.5	$\mathbf{L_2}$	7	$\mathbf{L_7}$	4.8
$\mathbf{L_f}$	1.25	$\mathbf{L_3}$	3.03	$\mathbf{W_8}$	6.23
$\mathbf{W_f}$	4.43	$\mathbf{W_3}$	4.27	$\mathbf{L_6}$	11.77
a	0.58	$\mathbf{L_4}$	1.87	**m**	1
b	0.87	$\mathbf{W_4}$	7.46	**n**	3
c	1.6	$\mathbf{L_5}$	3.64	**x**	2.75

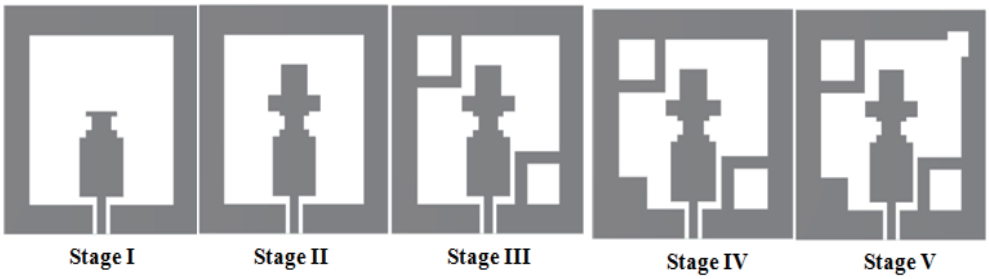

Figure 2. Various successive intermediate stages of the proposed CP antenna structure.

with linear polarization. In stage II, the patch is further modified by putting an inverted T-shaped structure on the top of it. In stage III, the ground is modified with two square shapes of the stub of the same width embedded at the two sides of the corner. Further improvement in the ARBW is obtained in stage IV, by putting a square-shaped structure on the left side of the ground. In this stage, S_{11} is improved, but axial ratio bandwidth at a higher frequency is less, so further improvement is done in the final design (stage V). In this stage, the ground is further modified by removing some portion from the top of the right side. Circular polarization is achieved by providing a 90° PD and equal magnitude.

Figures 3 and 4 depict the S_{11} (dB) and axial ratio versus frequency plots, respectively for different antenna prototypes of the designed CP antenna. During the analysis, it is observed that with the increasing number of iterations impedance bandwidth gets improved resulting in wider axial ratio bandwidth. In stage I and stage II there is no CP operation. Table 2 shows the comparison for the different antenna prototypes in terms of S_{11} (dB) and axial ratio. It can be observed from the Table that stage V (proposed design) provides better results in terms of S_{11} (dB) and axial ratio bandwidth.

2.3. Parametric Analysis

The impact of key parameters is presented in this section to study the effect of geometrical parameters of the proposed antenna on the magnitude of ($|S_{11}|$) and 3-dB ARBW. The parametric analysis gives the estimation of how more than one parameter affects a specific result. The following two parameters (dominate) are taken into consideration since these parameters mainly affect the performance of the proposed antenna.

2.3.1. Effect of Square Shape Stub Length (W_6)

When the square shape stub length of W_6 is varied from 1.8 mm to 4.3 mm in the interval of the 0.5 mm, the impact on $|S_{11}|$ and AR is depicted in Figs. 5(a) and 5(b), respectively. From the figure, it is analyzed that the lower sideband increases, and upper sideband decreases, but the optimal size of

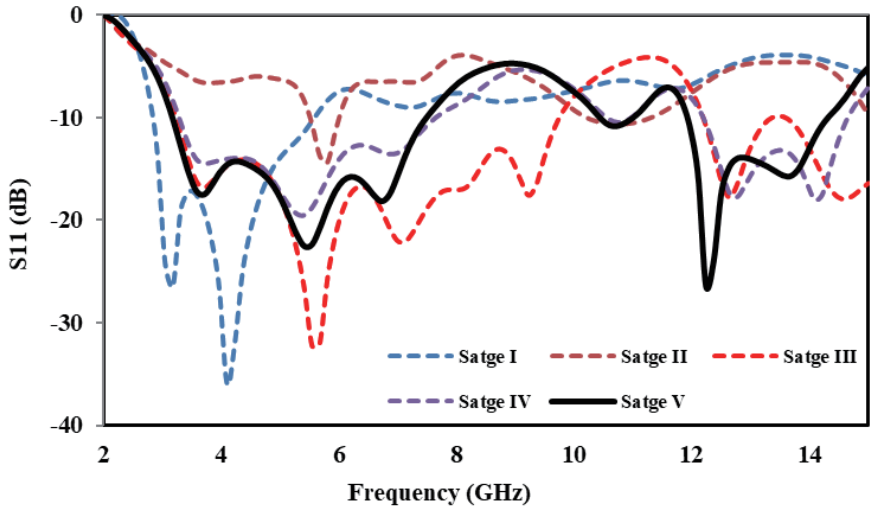

Figure 3. Simulated reflection coefficient (S_{11}) plot for different design stages.

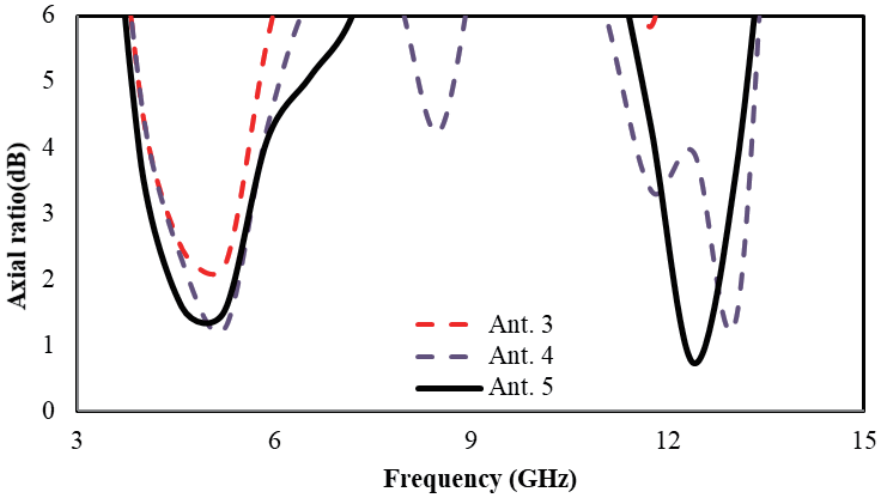

Figure 4. Simulated axial ratio plot for different stage.

Table 2. IMBW and 3-dB ARBW comparative analysis for different stages (I-V).

Design	IBW (GHz)	3-dB ARBW (GHz)	CP characteristics
Stage I	2.83–5.58	-	-
Stage II	5.51–6.01 10.21–11.29	-	-
Stage III	3.23–9.75 12.04–13.17	4.45–5.39	Single-band
Stage IV	3.28–7.66 12–14.76	4.41–5.61 12.64–13.16	Dual-band
Stage V	**3.16–7.5** **11.8–14.5**	**4.18–5.6** **11.86–12.96**	**Dual-band**

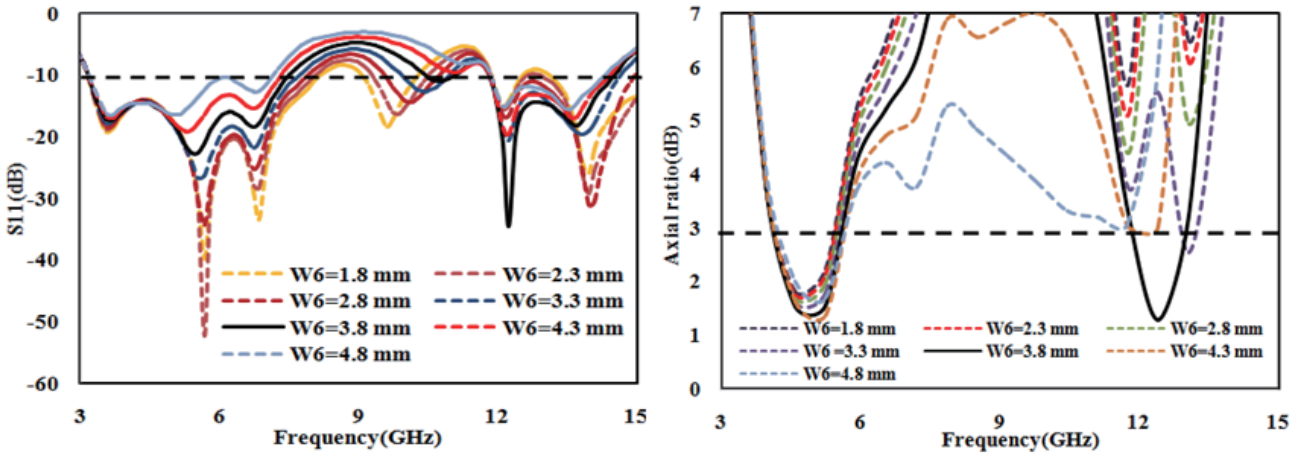

(a) (b)

Figure 5. Variation effect of W_6 on (a) $|S_{11}|$ and (b) Axial ratio.

$W_6 = 3.8$ mm is selected to get desired results. Similarly, for axial ratio curve, better 3-dB ARBW is achieved at $W_6 = 3.8$ mm, and the other values of stub wide axial ratio are achieved, but $|S_{11}|$ is not good. The observed value of $|S_{11}|$ and ARBW for varying parameters (W_6) is shown in Table 3.

Table 3. Variation effect of W_6 on Bandwidth and 3-dB ARBW.

Varying parameter (mm)	IBW (GHz)	3-dB ARBW (GHz)	CP characteristics
$W6 = 1.8$	3.15–8.18 11.8–12.5	4.21–5.41	Single-band
$W6 = 2.3$	3.16–8.06 9.27–10.5 11.8–12.6	4.21–5.44	Single-band
$W6 = 2.8$	3.16–7.91 11.82–14.95	4.2–5.48	Single-band
$W6 = 3.3$	11.8–14.64 3.17–7.73	4.19–5.53 12.9–13.1	Dual-band
W6 = 3.8	**3.16–7.47** **11.8–14.5**	**4.18–5.6** **11.86–12.96**	**Dual-band**
$W6 = 4.3$	3.17–7.32 11.8–14.4	4.21–5.66	Single-band
$W6 = 4.8$	3.18–7.15 11.84–14.31	4.29–5.67	Single-band

2.3.2. Effect of Grounded Rectangular Slot (n, m)

When the grounded rectangular slot of length (m, n) is varied, the impact on $|S_{11}|$ and AR is depicted in Figs. 6(a) and 6(b), respectively. Due to this slot, axial ratio bandwidth at the higher frequency gets improved. When the length n is increased from 2.5 mm to 5 mm with the interval of 0.5 mm, the length of m is varied from 0.5 mm to 3 mm. It is observed that when the value of n is increased, at a time

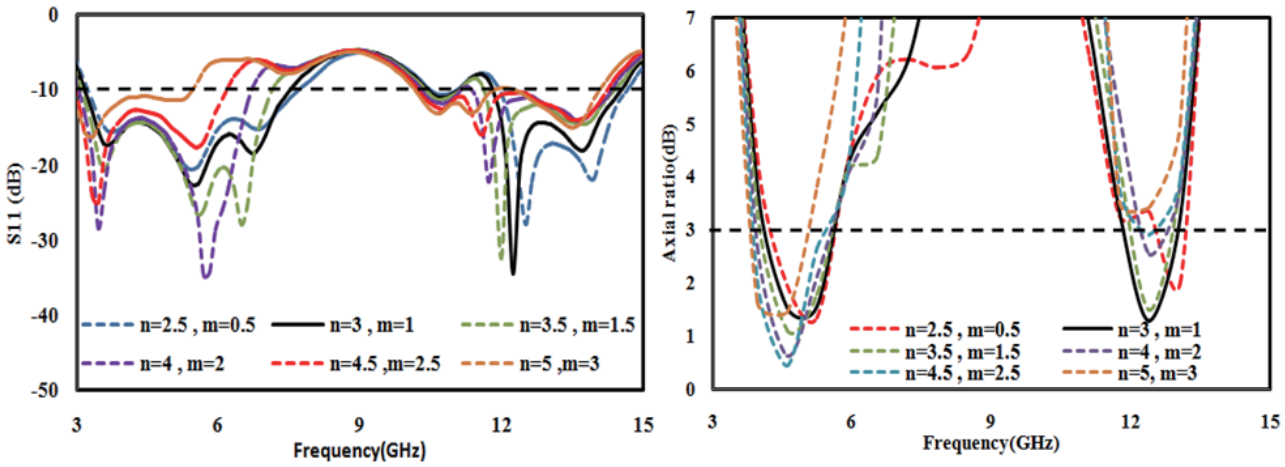

(a) (b)

Figure 6. Variation effect of slot (n, m) on (a) $|S11|$ and (b) Axial ratio.

only one desired antenna characteristic is achieved. The optimized values of m and n selected to obtain desired results are $m = 3$ mm and $n = 1$ mm, and the resultant values of $|S_{11}|$ and ARBW are shown in Table 4.

Table 4. Variation effect of slot length (n, m) on Bandwidth and 3-dB Axial ratio BW.

Varying parameter(mm)	IBW (GHz)	3-dB ARBW (GHz)	CP characteristics
$n = 2.5$, $m = 0.5$	3.22–7.69 11.94–14.64	4.32–5.16 12.56–13.13	Dual-band
n = 3, m = 1	**3.16–7.5** **11.8–14.51**	**4.18–5.6** **11.86–12.96**	**Dual-band**
$n = 3.5$, $m = 1.5$	3.09–7.13 11.6–14.38	4.05–5.58 12.04–12.81	Dual-band
$n = 4$, $m = 2$	3.02–6.7 11.34–14.31	3.92–5.54 12.28–12.63	Dual-band
$n = 4.5$, $m = 2.5$	2.94–6.16 10.22–14.22	3.87–5.4	Single-band
$n = 5$, $m = 3$	2.86–5.43 10.15–11.83 12.28–14.07	3.83–5.02	Single-band

2.4. Polarization Mechanism

To elucidate the polarization mechanism, the distribution of surface current vectors at 5 GHz and 12.5 GHz CP frequencies are illustrated in Figs. 7(a) and (b), respectively for different time instants $\omega t = 0°$, $90°$, $180°$, $270°$. It can be perceived that the surface current is predominately altered on the modified patch, inverted-L grounded strips, and stub having almost equal amplitudes and 90° PD leading to producing CP in a broadband range. In addition, it can be seen that at diverse time instants from 0° to 270°, the resultant current vector rotates in the anticlockwise direction inferring the sense

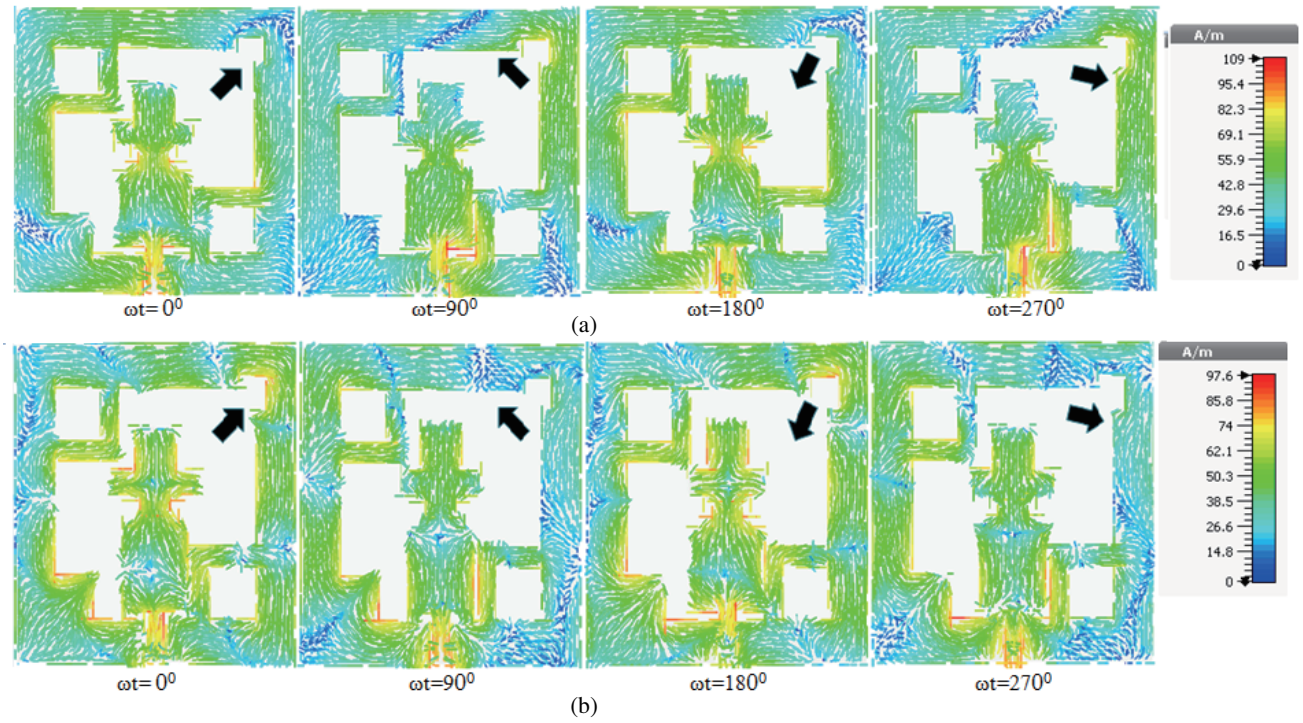

Figure 7. Simulated surface current distribution at (a) 5 GHz and (b)12.5 GHz.

of polarization as right-handed circular polarization (RHCP) in $+Z$ direction and LHCP (Left-hand circular polarization) wave in $-Z$ direction.

3. EXPERIMENTAL RESULTS AND DISCUSSION

A prototype has been fabricated using an easily available low-cost FR-4 substrate (shown in Fig. 8). The simulated S-parameter of the proposed antenna is evaluated using a full-wave CST microwave studio suite and measured using Agilent's E5071c vector network analyzer (VNA). The simulated and measured antenna performances ($|S_{11}|$ and axial ratio) are shown in Fig. 9 and Fig. 10, respectively. From Fig. 9, Fig. 10, and Table 5, it can be seen that there exist some sorts of discrepancies between the simulation-based results and experimental results. These marginal differences are attributed to different mesh sizes of the numerical technique of the simulator, errors in fabrication (fabrication tolerance), soldering, measurement, conductor losses, material losses, etc. Fig. 9 depicts the S_{11} results of the proposed antenna, which are verified in CST MWS and measurement. The proposed design provides the dual bands that have a lower band and upper band impedance bandwidth ranging from 3.16–7.5 GHz & 11.8–14.5 GHz by simulation tool and 3.18–7.1 GHz & 10.5–14.4 GHz using measurements, respectively.

Figure 10 depicts the simulated and measured axial ratios versus frequency plot of the proposed antenna. From this figure, it is seen that the designed antenna provides 3-dB ARBW of 4.18–5.6 GHz & 11.86–12.96 GHz using simulation and 4.2–5.4 GHz & 12.2–13.5 GHz using measurements.

The comparisons between results obtained by the simulation software CST and measurements in terms of S_{11} (dB) and 3-dB ARBW are shown in Table 5.

The radiation patterns simulated for XZ-plane ($Phi = 0°$) and YZ-plane ($Phi = 90°$) at frequencies 5 GHz and 12.5 GHz are depicted in Fig. 11. Figs. 11(a) and 10(b) show that the antenna gives RHCP in the $+Z$ direction and LHCP in the $-Z$ direction. At the 12.5 GHz, the radiations pattern is distorted due to the existence of higher operation modes.

Figure 12 depicted the gain versus frequency plot of the designed antenna. From this figure, it is observed that the designed antenna provides peak gain 3.8 dBi and 5 dBi in the lower and upper-frequency bands, respectively.

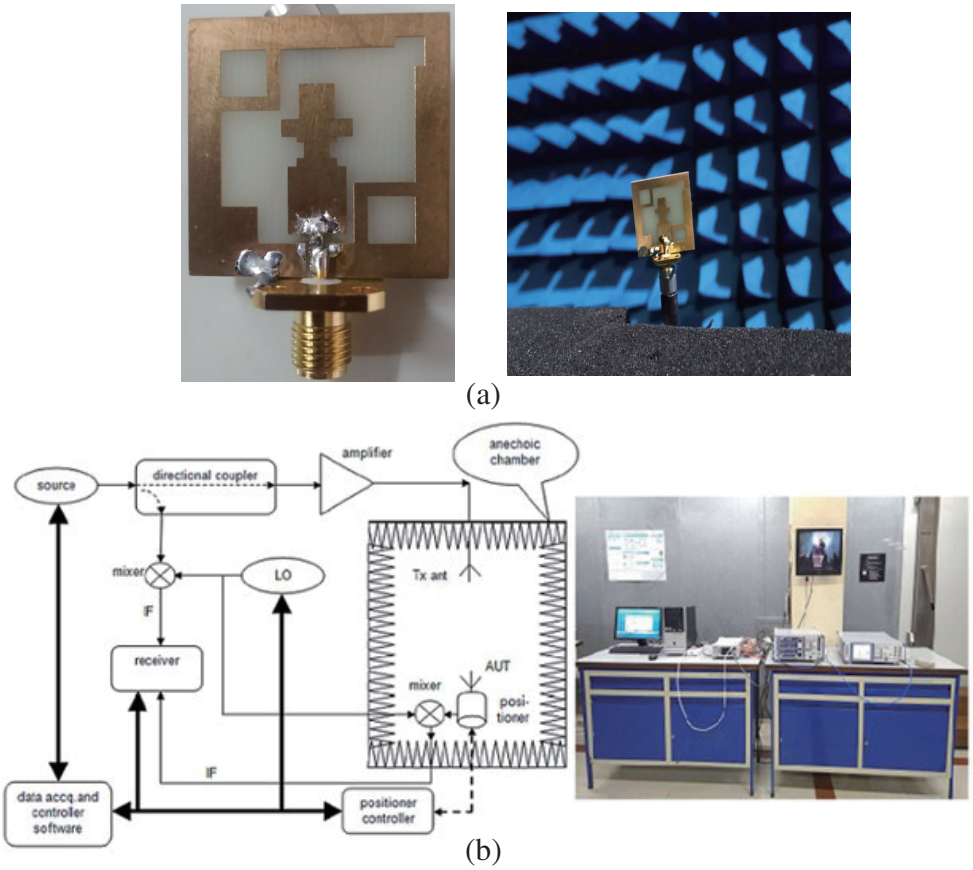

Figure 8. (a) Photograph of fabricated antenna with its measurement setup. (b) Schematic view of measurement setup and Photograph of measurement setup for anechoic Chamber facility.

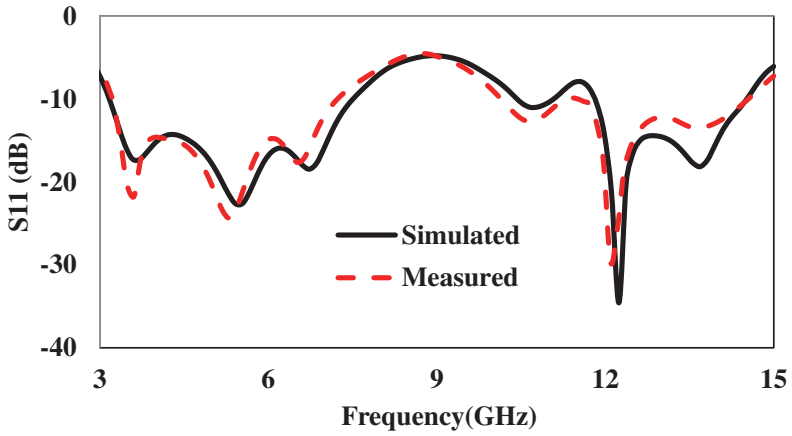

Figure 9. Simulation and measurement of S_{11} of proposed CP antenna.

The proposed CP antenna is compared with previously available structures in terms of percentage size reduction, IBW, 3-dB ARBW, and its CP response shown in Table 6. Here, antenna dimensions are related to the substrate material to compute the overall size of the antennas. It is analyzed that the proposed CP antenna is compact in size and provides large IBW and 3-dB ARBW as compared to reported work except [16]. In terms of electrical size, [16] is smaller than the proposed work, but other performance indices like IBW and ARBW are significantly improved.

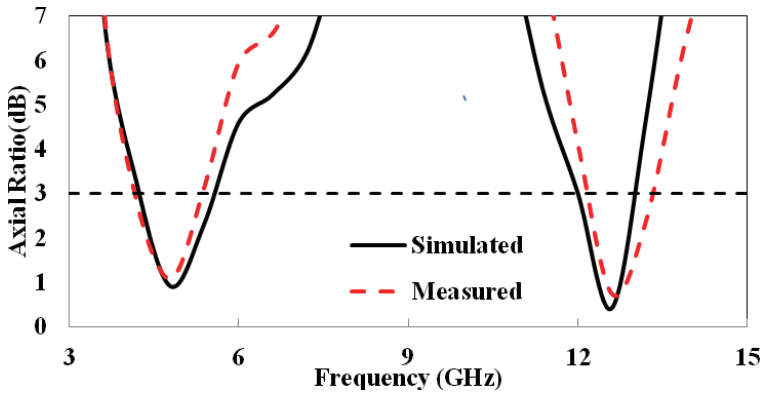

Figure 10. Simulated and measured axial ratio versus frequency plot of CP antenna.

Table 5. Comparison between S_{11} (dB) and 3-dB ARBW using different methods.

Methods	IBW (GHz)	3-dB ARBW (GHz)	CP characteristics
Simulated	3.16–7.5 11.8–14.5	4.18–5.6 11.86–12.96	Dual-band
Measured	3.18–7.2 10.5–14.5	4.2–5.4 12.2–13.5	Dual-band

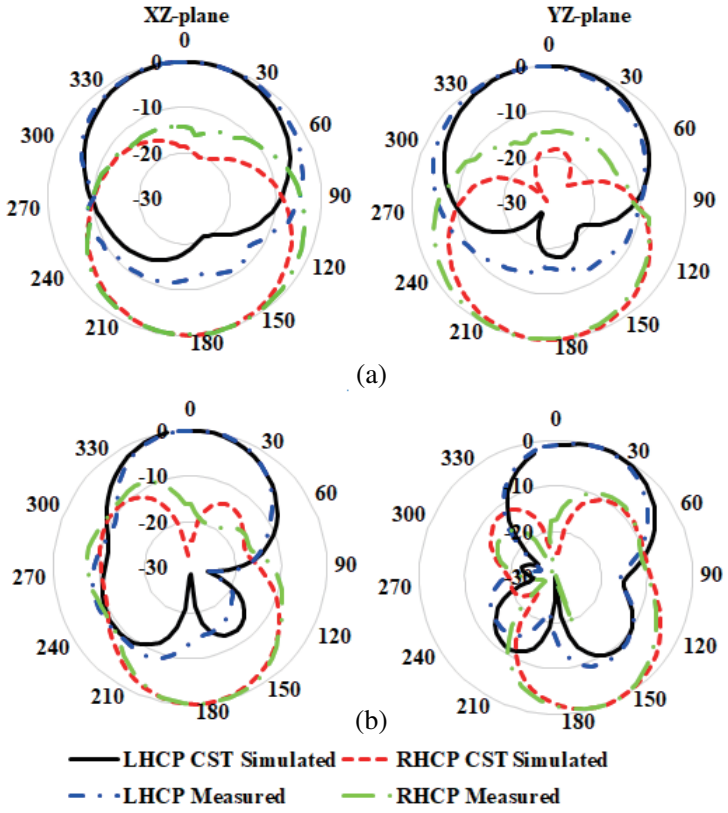

Figure 11. Simulated and measured radiation patterns at (a) 5 GHz and (b) 12.5 GHz.

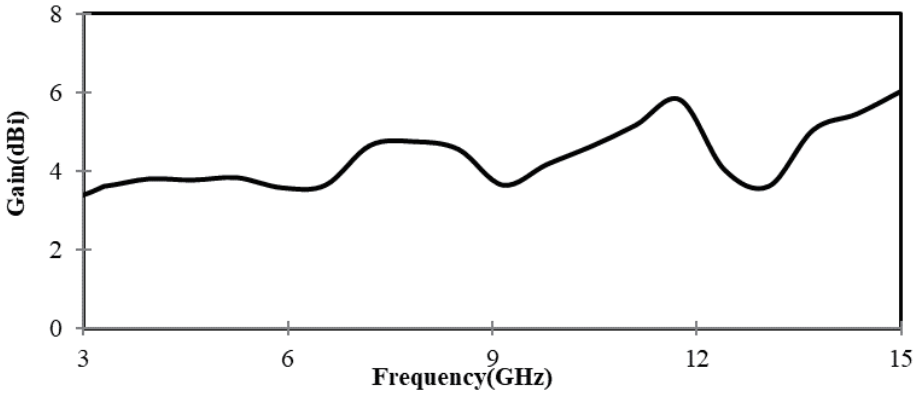

Figure 12. The measured Gain plot of the proposed CP antenna.

Table 6. Comparison of proposed CP antenna with other reported structures.

Ref.	Antenna Dimension (λ^2)	% Size Reduction	Impedance BW (GHz)	Axial ratio BW (GHZ)	CP characteristics
[10]	0.64×0.60	40.10	3.1–3.14 4.16–4.19	- -	LP
[11]	1.5×1.3	88.20	5.04–5.35 5.72–5.92	- -	LP
[12]	2×2	94.25	11.4–12.48 13.47–4.39	11.98 to 12.34 13.61 to 13.84	Dual-band
[13]	0.70×0.70	53.06	2.84–3.24 4.24–4.86	3.05 to 3.15 4.65 to 4.85	Dual-band
[14]	0.56×0.56	26.65	2.34–2.47 5.64–5.85	2.39–2.43 5.77–5.83	Dual-band
[15]	0.57×0.57	29.08	1.13–1.81	1.15–1.31 1.10–1.35	Dual-band
[16]	0.47×0.47	-4.1	1.15–1.65	118–13 1.48–1.59	Dual-band
Proposed Antenna	0.48×0.48	**-**	**3.16–7.5 11.8–14.5**	**4.18–5.6 11.86–12.96**	**Dual-band**

Note: λ is the wavelength at he lower resonant frequency, Abbreviation: LP-Linearly Polarized.

4. CONCLUSION

A dual-band CP antenna with stub and inverted L-strip loaded is designed, fabricated, and experimentally characterized. This antenna structure is optimized in size and easy to design. Also, the peak gain of the proposed antenna is 5 dBi, and it provides good radiation efficiency ($> 90\%$). The proposed design provides dual-bands, having measured IBW of 75.70% (3.2–7.1 GHz) and 32% (10.5–14.5 GHz), respectively. The measured axial ratio bandwidth for the two operating bands is 25% (4.2–5.4 GHz) and 10.11% (12.2–13.5 GHz), respectively. The proposed antenna has application in IMT advanced system in the frequency band of 4.6–5.2 GHz, MLS (5.150–5.350 GHz), BBDR (4.94–4.99 GHz), TV broadcast nonmilitary applications (11–12.20 GHz), broadcasting satellite (12.4–12.5 GHz), and 4.2–4.4 GHz radio altimeter.

REFERENCES

1. Wong, K.-L., *Compact and Broadband Microstrip Antennas*, John Wiley & Sons, 2002.
2. Jaiverdhan, A. K., M. M. Sharma, and R. P. Yadav, "Dual wideband circular polarized CPW-fed strip and slots loaded compact square slot antenna for wireless and satellite applications," *AEU — International Journal of Electronics and Communications (Elsevier)*, Vol. 108, 181–188, ISSN 1434-8411, 2019.
3. Davies, K., "Ionospheric radio propagation," NBS Monograph 80, 181, US Government Printing Office, Washington, DC, 1965.
4. Jaiverdhan, S., Sarthak, M. M. Sharma, and R. P. Yadav, "Epsilon-shaped circularly polarized strip and slot-loaded ultra-wideband antenna for Ku-band and K-band," *International Journal of RF and Microwave Computer-Aided Engineering*, Vol. 30, No. 5, e22142, 2020.
5. Jangid, M., M. M. Sharma, and Jaiverdhan, "CPW-fed dual-sense cross-shaped broadband circularly polarized antenna for wireless and satellite application," *Optical and Wireless Technologies. Lecture Notes in Electrical Engineering*, M. Tiwari, R. K. Maddila, A. K. Garg, A. Kumar, P. Yupapin, (eds), Vol. 771, Springer, Singapore, 2022.
6. Sze, J.-Y., C.-I. G. Hsu, Z.-W. Chen, and C.-C. Chang, "Broadband CPW fed circularly polarized square slot antenna with lightening shaped feedline and inverted-L grounded strips," *IEEE Trans. Antennas Propag.*, Vol. 58, No. 3, 973–977, 2010.
7. Pourahmadazar, J., C. Ghobadi, J. Nourinia, N. Felegari, and H. Shirzad, "Broadband CPW-fed circularly polarized square slot antenna with inverted-L strips for UWB applications," *IEEE Antennas Wireless Propag. Lett.*, Vol. 10, 369–372, 2011.
8. Felegari, N., J. Nourinia, C. Ghobadi, and P. J. Broadband, "CPW-fed circularly polarized square slot antenna with three inverted-L-shape grounded strips," *IEEE Antennas Wireless Propag. Lett.*, Vol. 10, 274–277, 2011.
9. Jaiverdhan, M. M. Sharma, R. P. Yadav, and R. Dhara, "Characteristic mode analysis and design of broadband circularly polarized CPW-fed compact printed square slot antenna," *Progress In Electromagnetics Research M*, Vol. 94, 105–118, 2020.
10. Li, Y., Z. Zhao, Z. Tang, and Y. Yin, "Differentially fed, dual-band filtering antenna with H-shaped slot," *Microw. Opt. Technol. Lett.*, Vol. 62, 448–452, 2020.
11. Chaturvedi, D., et al., "A nested SIW cavity-backing antenna for Wifi/ISM band applications," *IEEE Trans. Antennas Propag.*, Vol. 67, No. 4, 2775–2780, 2019.
12. Dong, Y. and T. Itoh, "Planar ultra-wideband antennas in Ku- and Kband for pattern or polarisation diversity applications," *IEEE Trans. Antennas Propag.*, Vol. 60, No. 6, 2886–2895, 2012.
13. Kandasamy, K., B. Majumder, J. Mukherjee, and K. P. Ray, "Dual-band circularly polarized split ring resonators loaded square slot antenna," *IEEE Trans. Antennas Propag.*, Vol. 64, No. 8, 3640–5, 2016.
14. Wang, W., C. Chen, S. Wang, and W. Wu, "Compact dual-band circularly polarized filtering patch antenna using dispersive delay line," *Microw. Opt. Technol. Lett.*, 1–9, 2020, https://doi.org/10.1002/ mop.32563.
15. Sun, Y. X., K. W. Leung, and J. Ren, "Dual-band circularly polarized antenna with wide axial ratio beamwidths for upper hemispherical coverage," *IEEE Access*, Vol. 6, 58132–58138, Oct. 2018.
16. Liu, H., C. Xun, S.-J. Fang, and Z. Wang, "Compact dual-band circularly polarized patch antenna with wide 3-dB axial ratio beamwidth for Beidou applications," *Progress In Electromagnetics Research M*, Vol. 87, 103–113, 2019.
17. CST Inc., CST Microwave Studio Suite v. 2021.